feature article

Photoacoustics for molecular imaging and therapy

Stanislav Y. Emelianov, Pai-Chi Li, and Matthew O'Donnell

Sound waves generated by light are the basis of a sensitive medical imaging technique with applications to cancer diagnosis and treatment.

Stanislav Y. Emelianov is an associate professor in the department of biomedical engineering at the University of Texas at Austin. **Pai-Chi Li** is a professor in the Institute of Biomedical Electronics and Bioinformatics and the department of electrical engineering at National Taiwan University in Taipei. **Matthew O'Donnell** is a professor in the department of bioengineering and dean of the college of engineering at the University of Washington in Seattle.

Children often marvel at the power of lightning and thunder, a dazzling interplay between light and sound. With modern nanomaterials, photonics, and ultrasonics technologies, researchers are now translating the wonders of sound produced by optical interactions at the nanoscale into photoacoustic systems. Those systems have the potential to provide cost-effective molecular imaging and therapy in medicine.

Light can be used to both generate and detect sound. Several physical mechanisms can be used for sound generation, but the most common is photoacoustics. The photoacoustic effect was discovered more than 125 years ago by Alexander Graham Bell.[1] He created a device he called the photophone, and several derivative devices such as the spectrophone shown in figure 1a, in which a rotating thin disk emitted sound when exposed to a focused beam of light. Absorbed optical energy heated part of the disk, which was physically displaced via thermal expansion. Displacements were time modulated by the disk's rotation, which resulted in a sound wave equal in frequency to the mechanical rotation. The acoustic wave was detected with a stethoscope.

Light has also been used to detect sound. With the invention and rapid adoption of the laser in the 1960s, a number of optoacoustic imaging systems have been proposed based on coherent optical detection of ultrasound.[2] They were not developed into practical imaging systems, because they had poor sensitivity compared with alternate approaches that used piezoelectric detection. More recent work, however, has demonstrated that acoustically coupled resonant optical devices, such as the one shown in figure 1b, can be as sensitive as the best piezoelectric detectors without requiring direct electrical connections.[3]

The focus of this article is on photoacoustic imaging systems in which pulsed light propagates into a biological medium and is differentially absorbed in space, creating a spatial distribution of sound sources imaged by an array of acoustic sensors. Optoacoustic sensors have been used for those systems, but here we focus on photoacoustic imaging in medicine without reference to any specific detector technology.

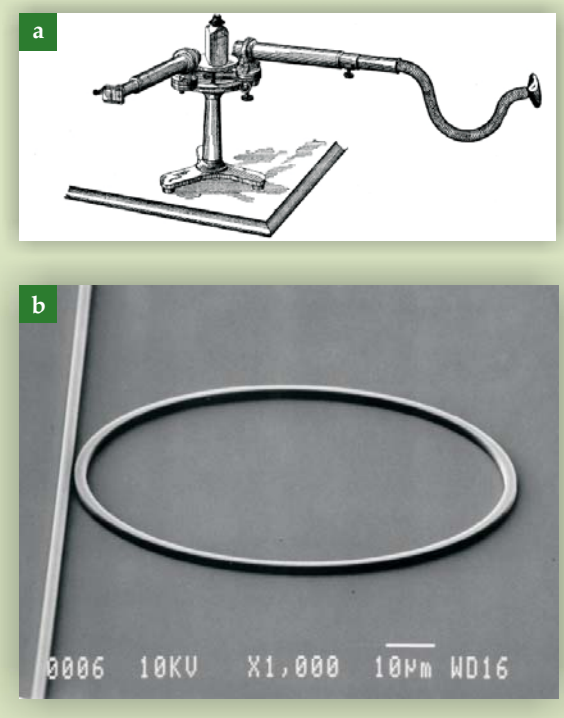

Figure 1. (a) Using a device called a spectrophone, Alexander Graham Bell demonstrated that light can generate sound. The rotating object in the middle absorbs energy from a focused beam of light. The resulting time-modulated thermal expansion can be detected with a stethoscope. (From ref. 1.) **(b)** A waveguide ring resonator uses light to detect sound. Light is coupled from the straight waveguide on the left into the micro-ring when its effective wavelength is an integral fraction of the ring circumference. Acoustic waves distort the waveguide dimensions and alter the observed resonance spectrum. (From ref. 3.)

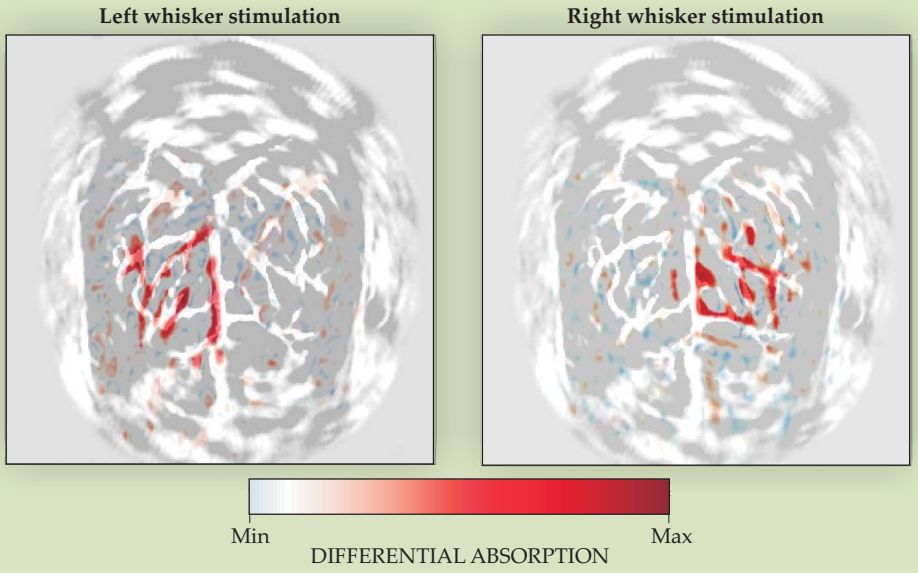

Figure 2. Photoacoustic images showing oxygen utilization in the brain of a rat when its whiskers are stimulated. Each panel shows the differential absorption between the unstimulated brain and the brain during left or right whisker stimulation. The images were taken at a wavelength at which the optical absorption spectra of oxygenated and deoxygenated hemoglobin differ, so the regions of high differential absorption indicate regions of oxygen utilization. (Adapted from ref. 8.)

Why photoacoustics in medicine?

Since Antoni van Leeuwenhoek's discoveries in the 17th century, optical imaging has been instrumental in the life sciences. A wide range of optical techniques are routinely used in biomedicine,[4] often in conjunction with fluorescence or coupled-fluorescence agents that enable the optical probing of specific molecular events in biological systems. Optical imaging systems coupled with molecular contrast agents are extremely sensitive tools for studying living systems. But few of those tools have been translated into the clinic.

The key limitation for clinical applications is optical absorption and scattering by tissue. At near-IR wavelengths (2000–3000 nm), water is the dominant absorber, so light penetration depth is limited to 0.1–1 mm. In the UV region near 300 nm, the absorption depth is shallow due to absorption by cellular macromolecules. Between 650 nm and 1300 nm, absorption by water, hemoglobin, and lipids is lowest, so light can penetrate to several centimeters, and contrast between tissue components remains high. That wavelength range is often referred to as the "therapeutic window" or "diagnostic window."

Light scattering is still an issue within that spectral window. For techniques that require coherent light, penetration into tissue is limited to 1–2 mm, but high spatial resolution is maintained—typically 1–10 μm. In contrast, incoherent and partially coherent techniques allow penetration to several centimeters, but their spatial resolution is typically reduced to 3–10 mm. There is great need for an imaging technique with the molecular sensitivity of optics but with penetration and spatial resolution typical of other clinical imaging modalities.

Photoacoustic imaging is such a technique. It was first proposed as a medical imaging modality nearly 30 years ago by Theodore Bowen at the University of Arizona.[5] Subsequent work by Alexander Oraevsky,[6] Robert Kruger,[7] Lihong Wang,[8] and others has built on recent advances in pulsed laser technology to produce photoacoustic images with the same high spatial resolution achieved by ultrasound imaging.

Optical absorption, the primary contrast mechanism in photoacoustic imaging, is not shared by any other clinical or biomedical imaging system, including optical imaging, ultrasonic imaging, x-ray- and gamma-ray-based imaging, and magnetic resonance imaging. For example, contrast in optical imaging is determined primarily by refractive index and in ultrasound imaging by heterogeneities in mechanical properties such as density and compressibility.

The images in figure 2, collected by Wang and colleagues,[8] demonstrate the potential of photoacoustics to image molecular properties at high resolution in functional studies of the brain. The difference in the optical absorption spectra of oxygenated and deoxygenated hemoglobin was exploited to image oxygen utilization in the brain of a rat undergoing whisker stimulation. The studies by Wang and colleagues demonstrated that photoacoustic imaging can monitor molecular properties directly related to oxygen utilization. From their work, photoacoustics can be extended as a general-purpose tool for molecular imaging and therapy.

Imaging systems

The basic principle of all photoacoustic (and, more generally, thermoacoustic) techniques is that the absorption of electromagnetic energy causes a change of thermal state that leads to a change in temperature, density, and possibly pressure.[5] In photoacoustic imaging, acoustic waves are produced by pulsed laser light.[6] For biomedical applications, photoacoustic generation is due to the photothermal effect: Heat deposited by absorbed light produces acoustic waves through thermal expansion.[9] Temperature elevations are very small—for example, if skin is irradiated with the maximum permissible exposure of laser light, tissue surfaces are warmed by a few hundredths of a degree, and the acoustic wave has an amplitude of hundreds of millibars.

Consider plane-wave illumination of an object by a pulsed laser source of high peak power but very low duty cycle—for example, a 10-ns pulse produced at a repetition rate of 20 Hz. If energy is absorbed faster than it can diffuse away, a local volume with elevated absorption is heated by the laser pulse, and a local acoustic transient is generated. The magnitude and shape of the acoustic transient depend on the duration of the laser pulse.

Under conditions typical for biomedical imaging, the photoacoustic wave equation is

$$\left(\nabla^2 - \frac{1}{v_s^2}\frac{\partial^2}{\partial t^2}\right) p = -\frac{\Gamma}{v_s^2}\frac{\partial H}{\partial t}, \qquad (1)$$

where p is pressure, v_s is the longitudinal wave speed in the

medium, Γ is the dimensionless Grüneisen parameter

$$\frac{\beta v_s^2}{C_p}, \qquad (2)$$

β is the thermal coefficient of volume expansion, C_p is the heat capacity at constant pressure, and H is the heating function representing thermal energy deposited per unit volume and per unit time.[9,10] Absorbed laser light and the corresponding temperature rise generate the source term in the acoustic wave equation. Localized regions of high optical absorption act as sources of propagating acoustic waves.

Under a so-called stress confinement condition—in which the duration of the laser pulse is less than a characteristic confinement time—the amplitude of the acoustic wave launched by an optical absorber depends only on the total amount of energy absorbed, not on its time profile, and so is given by $\Gamma\mu_a F$, where μ_a is the optical absorption coefficient and F is the optical fluence at the absorber. The acoustic wave's specific shape is determined by the boundary conditions for all optical absorbers heated by the laser. In the limit of highly localized, instantaneous absorption, the acoustic pulse shape is approximated by the time derivative of the optical pulse.[10]

Propagating acoustic waves created by each optical pulse can be detected and recorded by an array of ultrasonic transducers, as illustrated in figure 3, and rapidly reconstructed to produce real-time images of the source distribution. If optical illumination and acoustic detection systems are properly designed, a complete 2D or 3D image can be produced from a single laser pulse. In addition, ultrasonic and photoacoustic imaging can share array and receiver electronics and can therefore be combined to obtain photoacoustic and ultrasonic images of the same object in rapid succession at real-time (that is, video) rates.

Ultrasonic imaging is the mostly commonly used real-time clinical modality capable of 2D and 3D images.[11] Spatial resolution is directly related to the acoustic frequency, which is typically 1–20 MHz, and corresponds to acoustic wavelengths of 1.5 mm to 75 μm. The ultrasonic attenuation coefficient is also nearly linear with operating frequency, so there is a direct tradeoff between spatial resolution and penetration. Submillimeter spatial resolution is typical up to penetration depths of about 15 cm, and better than 100-μm resolution is possible at depths up to several centimeters. Contrast in ultrasonic images is related to mechanical characteristics of soft tissue. Since mechanical properties are not directly related to molecular function, ultrasonic systems provide mostly anatomical images and physiological measurements related to blood flow and tissue elasticity. Therefore, when ultrasonic and photoacoustic systems are combined, both morphology (that is, anatomy) and function (for example, blood oxygenation as illustrated in figure 2) can be imaged simultaneously. Furthermore, multimodal imaging can be extended to cellular and molecular events.

Figure 4 shows a block diagram of a typical photoacoustic imaging system. To achieve the spatial resolution and field of view required for biomedical applications, most systems use nanosecond pulsed lasers such as Q-switched neodymium-doped yttrium aluminum garnet, alexandrite, and tunable pulsed lasers or high-peak-power pulsed diode lasers. The laser beam's energy is typically delivered to the tissue via an optical fiber or a set of optical fibers tightly bundled on the laser-head side and distributed around the ultrasonic transducer on the other end. Each fiber may be attached to an optical diffuser positioned to produce nearly uniform optical illumination of the image plane probed by the transducer array. Light scattering in tissue also helps to spatially homogenize the laser irradiation. If a single fiber is used, the laser beam is distributed around the transducer and into the tissue using an assembly of lenses, prisms, and mirrors.

Molecular imaging applications

Molecular imaging marries molecular biology tools with in vivo imaging technologies. The goal is to obtain images directly related to the activity of a molecular process in the body. Typically, sensitive contrast agents are targeted to biomolecular markers of disease, so that image contrast is proportional to the concentration of the biomarker. For example, molecular imaging of cancer cells commonly targets surface molecules that encourage growth and metastasis and are important in the prediction of clinical outcome and treatment response of anticancer drugs. Imaging cancer lesions while simultaneously obtaining information at a molecular level on oncogenic proteins is of great clinical significance. For photoacoustic molecular imaging, gold nanoparticles with high optical absorption coefficient can be targeted to specific cancer biomarkers, which allows the noninvasive detection and monitoring of cancer at the molecular level.

Gold nanoparticles have been used for various biomedical applications,[12] including as contrast agents for photoacoustic imaging.[13] One intriguing property is that their absorption spectra are geometry dependent. Size affects surface plasmon absorption, with the result that the peak optical absorption redshifts with increasing particle size. Gold nanospheres with diameters of tens of nanometers have absorption peaks around 550 nm.[14] For gold nanorods, the peak absorption wavelength depends only weakly on diameter but increases strongly with aspect ratio. A gold nanorod with an aspect ratio of 4

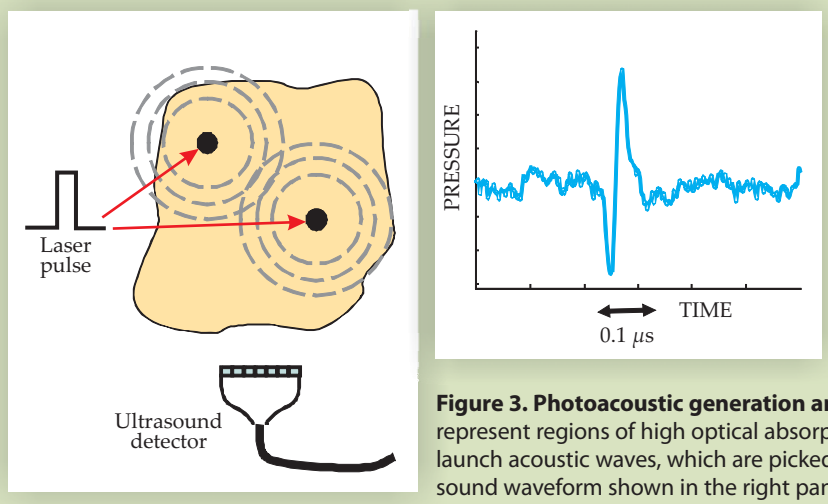

Figure 3. Photoacoustic generation and detection. Black dots in the left panel represent regions of high optical absorption. When heated by a laser pulse, they launch acoustic waves, which are picked up by an ultrasound detector. The ultrasound waveform shown in the right panel is approximately proportional to the time derivative of the optical pulse.

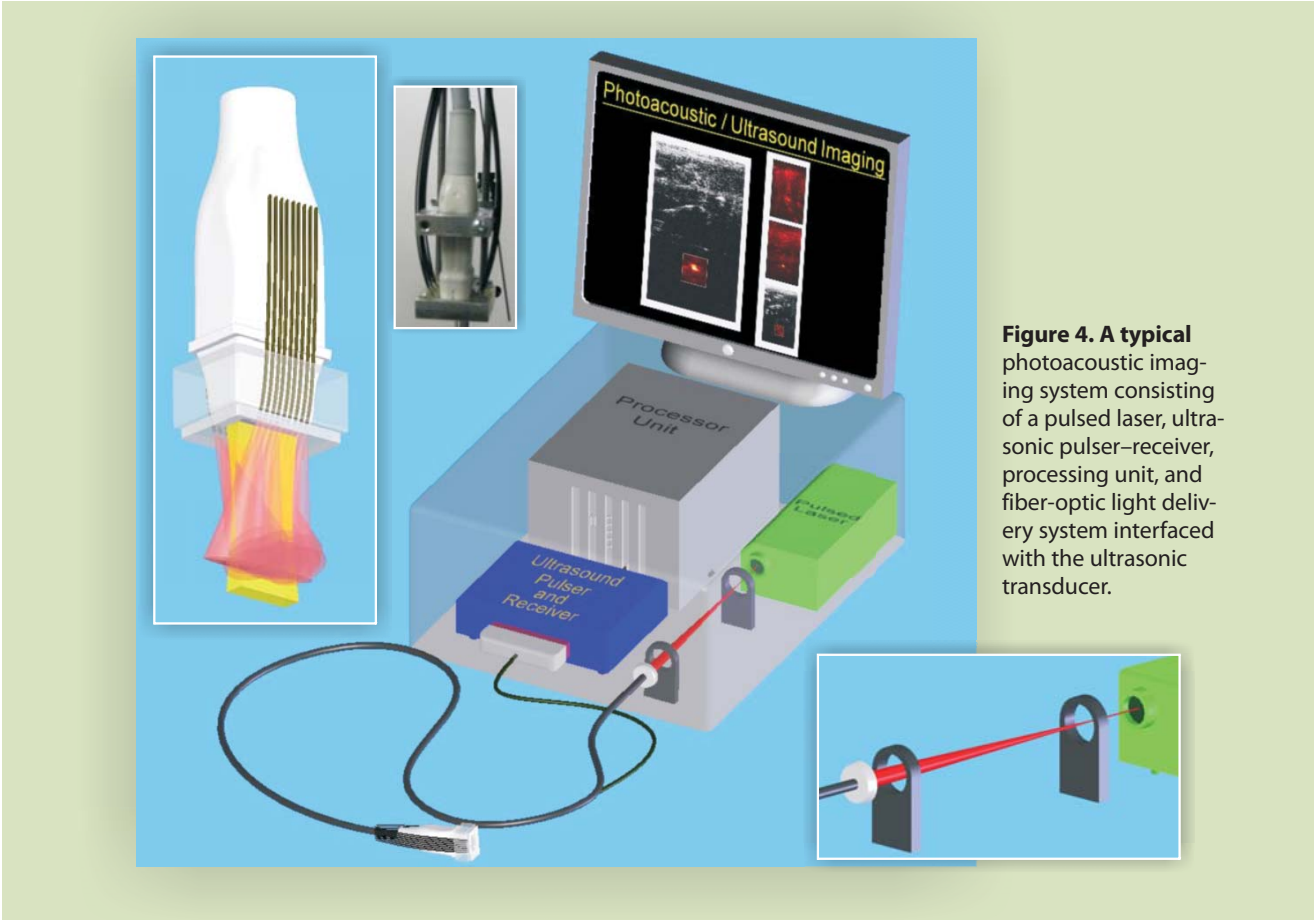

Figure 4. A typical photoacoustic imaging system consisting of a pulsed laser, ultrasonic pulser–receiver, processing unit, and fiber-optic light delivery system interfaced with the ultrasonic transducer.

has its absorption peak at a wavelength slightly greater than 800 nm—well within the diagnostic window.

Targeting gold nanoparticles to specific cells helps in early cancer detection due to the large difference in optical absorption between the particles and tissue. To target a nanorod to a specific biomarker, or antigen, an antibody to the biomarker is affixed to the nanorod surface. The nanorods then accumulate in or on the targeted cells in proportion to the number of biomarkers present. The photoacoustic signal increases with increased nanoparticle concentration, so contrast in a photoacoustic image is proportional to biomarker concentration. In addition, different molecules can be targeted with nanorods of different aspect ratios[15] so that an array of biomarkers can be imaged simply by changing the optical wavelength.

Binding efficacy between cells and the bioconjugated gold nanorods can be examined by transmission electron microscopy. Figure 5a shows gold nanorods under TEM, and figure 5b shows a 70-nm-thick slice of a cancer cell with bioconjugated gold nanorods attached to the cell surface. The nanorods are conjugated with an antibody to the human epidermal growth factor receptor 2 (HER2), a membrane-bound protein greatly overexpressed in several forms of cancer. About 5000 nanorods are estimated to have been attached to the whole cell. In comparison, for a highly homogeneous sample of gold nanorods, as few as 10 particles can be detected photoacoustically in the resolution cell of a typical image. Figure 5c shows cell internalization of bioconjugated gold nanorods after surface binding to the epidermal growth factor receptor (EGFR), another membrane-bound protein overexpressed in several cancers.[16]

Photoacoustic and ultrasonic images can be combined and displayed simultaneously. With bioconjugated gold nanoparticles as the molecular probe, the photoacoustic image identifies a specific molecular process, while the ultrasonic image provides anatomic information. Ultrasonic images are often displayed on a grayscale, similar to the B, or brightness, mode of clinical ultrasound (see the article by Carr Everbach in PHYSICS TODAY, March 2007, page 44), and the photoacoustic images are displayed in pseudocolors. When gold nanorods with different aspect ratios are used to target several biomarkers, the photoacoustic images acquired at different laser wavelengths can be simultaneously displayed in pseudocolors of different hues.

Figures 5d and 5e show a photoacoustic–ultrasonic image of an oral epidermoid carcinoma tumor subcutaneously implanted in a mouse. The underlying ultrasonic images show the mouse's skin. Figure 5d shows the image before injection of targeted gold nanoparticles; the photoacoustic signal is weak and generally below the display's dynamic range. After injection of nanoparticles, the tumor appears as a well-defined bright spot, as shown in figure 5e.

Molecular therapy

The high target specificity of molecular contrast agents can also be used for molecular therapy. For example, in photothermal cancer therapy, radiant energy is converted to thermal energy that can destroy cancer cells. Its effectiveness is directly related to how well the heating can be localized to tumor cells. Just like in molecular imaging, localized regions of high optical absorpton coefficient can be created by molec-

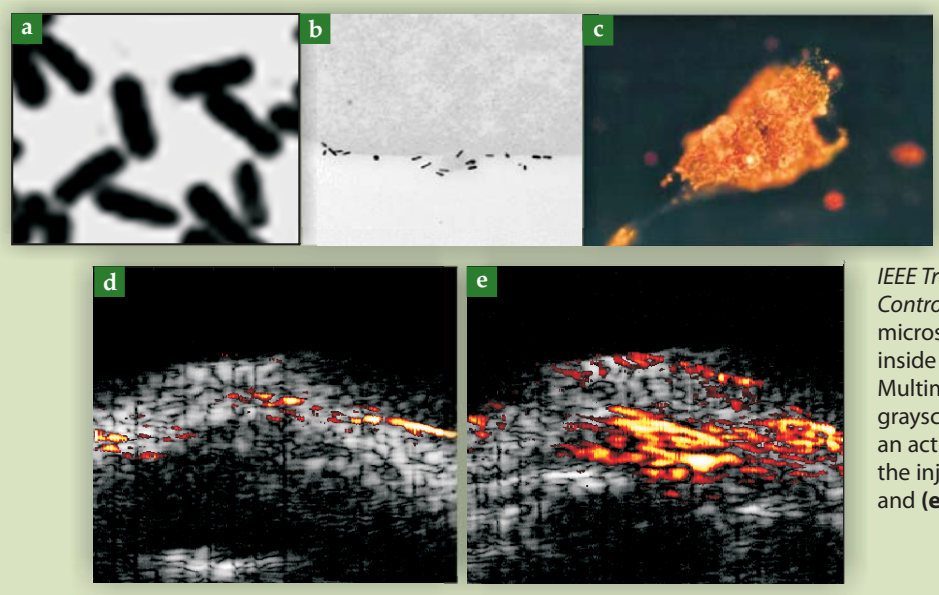

Figure 5. Transmission electron microscopy images of gold nanorods: **(a)** in isolation and **(b)** on the surface of a cancer cell (adapted from P.-C. Li et al., *IEEE Trans. Ultrason. Ferroelectr. Freq. Control* **54**, 1642, 2007); **(c)** Optical microscopy image of gold nanorods inside a cancer cell (from ref. 16); Multimodality images (ultrasonic in grayscale, photoacoustic in color) of an active tumor in a mouse **(d)** before the injection of targeted gold nanorods and **(e)** after.

ular targeting of photothermal contrast agents, which greatly increases the therapy's effectiveness and minimizes heat damage to neighboring healthy tissue. In addition, the same agents can be used to produce photoacoustic images that can help to optimize therapeutics.

In a typical procedure, molecularly targeted photoabsorbers, such as the gold nanoparticles described previously, are delivered to cancerous tissue. Laser irradiation then heats and destroys the tumor. For therapy to be successful, the tumor must first be identified and diagnosed. Then, uptake and sufficient accumulation of photoabsorbers in the tumor must be confirmed. During the treatment, the temperature increase must be noninvasively tracked to ensure that cancerous tissue is being killed and surrounding healthy tissue is not. Finally, the treatment outcome must be monitored to verify that the tumor has been completely destroyed and to identify any possible resurgence.

Simultaneous photoacoustic and ultrasonic imaging can help efficiently deliver molecularly targeted photothermal therapy. Before a procedure, the tumor is imaged to develop an appropriate treatment plan. During therapy, real-time images help guide photothermal therapy by tracking the uptake of photoabsorbers. Once enough photoabsorbers have accumulated in the tumor, the temperature rise can be mapped using multimodal imaging. After therapy, multimodal imaging can be used to accurately assess both short- and long-term treatment outcomes.

The dimensionless Grüneisen parameter, one factor in the expression for the photoacoustic pressure amplitude, is temperature dependent.[17] Photoacoustic images can therefore be used to monitor changes in tissue temperature during photothermal therapy, as shown in figure 6. A tumor-bearing mouse was injected with gold nanorods targeted to the tumor. A continuous-wave laser tuned to the nanorods' maximum absorption wavelength provided the therapeutic source, and photoacoustic imaging was performed with a pulsed laser operating at the same wavelength. One hour after nanorods were injected, photothermal therapy was applied for three minutes. Ultrasonic and photoacoustics-based thermal images acquired after 60, 120, and 180 seconds of laser irradiation show a gradual increase in temperature as therapy progresses—at the end of the three minutes, the

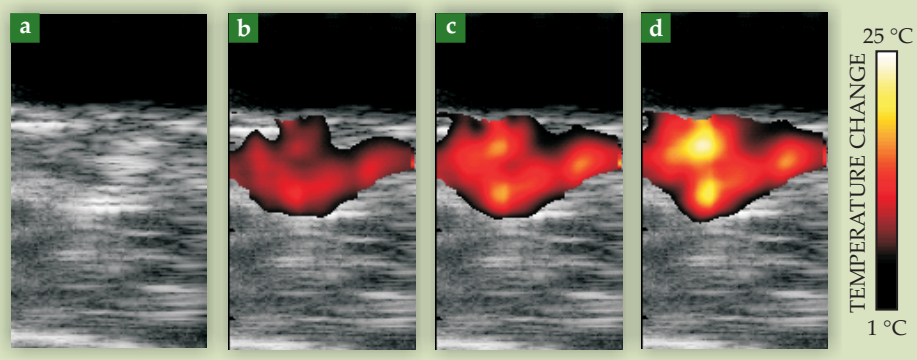

Figure 6. Photoacoustic imaging of temperature during photothermal cancer therapy of a tumor-bearing mouse. The mouse was injected with optically absorbing gold nanorods targeted to a protein in the cancer cells. The tumor region was then irradiated with continuous-wave laser light at the nanorods' peak absorption wavelength. Images taken after **(a)** 0, **(b)** 60, **(c)** 120, and **(d)** 180 seconds of treatment show the temperature rise in the tumor. Each image represents a 10.5-mm by 20-mm field of view.

tumor temperature was elevated by more than 20 °C. Histological evaluation after the procedure confirmed that the tumor had indeed been thermally damaged—evidence of the significant role that photoacoustics can play in optimally delivering molecular therapy.

Prospects

The photoacoustic effect has been used in the physical sciences for more than 125 years. With significant advances in optical, ultrasonic, and nanomaterials technologies in the past decade, photoacoustics is also becoming an important tool for diagnostics and therapy. Systems have been recently developed that integrate photoacoustic and ultrasonic imaging. As bioconjugated contrast agents become more specific and sensitive, combined ultrasonic and photoacoustic imaging may provide the molecular sensitivity of optical techniques but with the spatial resolution and penetration depth of ultrasonic imaging. These systems can present simultaneous images showing morphology and molecular function at real-time frame rates appropriate for clinical applications.

Drawing on the same principles used for photoacoustic molecular imaging, integrated ultrasonic–photoacoustic systems can also help to optimize the delivery of molecularly targeted photothermal therapy. For example, in cancer treatment, ultrasound imaging can identify tissue heterogeneities and provide anatomical information about a tumor. Complementary photoacoustic images, based on uptake of labeled nanoparticles, may help to define the tumor boundaries and determine when enough of the particles have been delivered for therapy to be effective. Finally, photothermal therapy can be initiated and guided using photoacoustic and ultrasonic imaging.

The future for integrated ultrasonic–photoacoustic imaging and therapy systems is bright. They combine many desirable properties of optical and ultrasonic systems and may become one of the primary clinical delivery vehicles for molecular imaging and therapy. Miniaturization of the imaging devices, particularly the scan head, will also facilitate new clinical applications such as intravascular imaging and image guidance for minimally invasive surgeries. Finally, new photoacoustic probes that mimic fluorescence-based optical probes are rapidly being developed for clinical applications.

References

1. A. G. Bell, *J. Franklin Inst.* **111**, 401 (1881).
2. H. Berger, in *Acoustical Holography*, vol. 1, A. F. Metherell, H. M. A. El-Sum, L. Larmore, eds., Plenum Press, New York (1969), p. 27.
3. S. Ashkenazi et al., in *Photoacoustic Imaging and Spectroscopy*, L. V. Wang, ed., CRC Press, Boca Raton, FL (2009), p. 223.
4. R. Weissleder, M. J. Pittet, *Nature* **452**, 580 (2008).
5. T. Bowen, *Proc. IEEE Ultrason. Symp.* **2**, 817 (1981).
6. A. A. Oraevsky et al., in *OSA Proceedings on Advances in Optical Imaging and Photon Migration*, R. R. Alfano, ed., Optical Society of America, Washington, DC (1994), p. 161.
7. R. A. Kruger, P. Liu, *Med. Phys.* **21**, 1179 (1994).
8. X. Wang et al., *Nat. Biotechnol.* **21**, 803 (2003).
9. A. C. Tam, *Rev. Mod. Phys.* **58**, 381 (1986).
10. G. J. Diebold, T. Sun, *Acustica* **80**, 339 (1994).
11. K. Kirk Shung, *Diagnostic Ultrasound: Imaging and Blood Flow Measurements*, CRC Press, Boca Raton, FL (2005).
12. T. A. Taton, C. A. Mirkin, R. L. Letsinger, *Science* **289**, 1757 (2000); A. K. Boal et al., *Nature* **404**, 746 (2000).
13. P.-C. Li et al., *Opt. Lett.* **30**, 3341 (2005); S. Mallidi et al., *Opt. Express* **15**, 6583 (2007).
14. S. Link, M. A. El-Sayed, *J. Phys. Chem. B* **103**, 8410 (1999).
15. P.-C. Li et al., *Opt. Express* **16**, 18605 (2008).
16. X. Huang et al., *J. Am. Chem. Soc.* **128**, 2115 (2006).
17. J. Shah et al., *J. Biomed. Opt.* **13**, 034024 (2008).

■